ISSN 1392 – 1231. CHEMINĖ TECHNOLOGIJA. 2016. Nr. 1 (67)

Influence of silica fume on the workability and hydration process of ultra-high performance concrete

E. Šerelis, V. Vaitkevičius, V. Kerševičius
Kaunas University of Technology
Faculty of Civil Engineering and Architecture
Studentu Str. 48, LT-51367 Kaunas, Lithuania
E-mail: evaldas.serelis@ktu.lt

crossref http://dx.doi.org/10.5755/j01.ct.67.1.15825

Received 19 May 2016; Accepted 16 June 2016

The present article reviews the influence of silica fume on the workability and hydration process of ultra-high performance concrete (UHPC). Silica fume, also known as microsilica (MS) or condensed silica fume, is a by-product of the production of silicon metal or ferrosilicon alloys. Silica fume is one of the most effective pozzolanic additives which could be used for ultrahigh-performance and other types of concrete. According to the literature review, it is not entirely clear which amount of silica fume is optimal, how silica fume affects the hydration process; although the literature is rich in reporting on silica fume, however, most of the scientists are concentrated on workability and compressive strength. The purpose of this research is to extend knowledge on the workability and hydration process of ultra-high performance concrete affected by different amounts of silica fume. For investigation, slump, viscosity, qualitative and quantitative XRD analysis and compression strength tests were applied. The hydration time was reduces by 4.5 hours, and the compressive strength was increased by 30 % (from 95 MPa up to 127 MPa).

Key words: compressive strength, silica fume, ultrahigh performance concrete, XRD.

Introduction

Over the past few decades, significant advances in research on cementitious materials have been made, which led to developing a new class composition material with improved strength and durability properties. Probably the best durability and compressive strength properties could be attributed to the ultra-high performance concrete (UHPC). In Lithuania, UHPC is known as the concrete which has a compressive strength over 100 MPa [1]. However, by a adding proper amount of necessary materials, the compressive strength could be increased up to 200 MPa [2–4]. Chemical admixtures are very important additives which help to reduce the water-to-cement ratio below 0.30, and pozzolanic additives (fly ash, silica fume, ground-granulated blast-furnace slag, etc.) are very beneficial to gain additional mechanical strength during the further hydration process. The most common pozzolanic material used in the UHPC is silica fume [5, 6]. The interaction of silica fume with reactive materials is very complicated and greatly affects the workability and hydration of cementitious materials. A deeper research is required to proper by understand the interaction of silica fume with the ultra-high performance concrete.

Most authors denote that silica fume works on two levels: physical and chemical. The physical effect of silica fume on the concrete is due to its more than 100 times smaller particles than of cement. Fine grains can fit into the space between cement grains in the same way as sand can fill the space between coarse aggregates [7, 8]. A proper particle packing and the optimal amount of silica fume is required in order to get the densest structure with the highest compressive strength and the resistivity to the aggressive environment. The chemical effect is due to the high surface area of amorphous silica which tends to react with portlandite and form additional C-S-H [9, 10]. Although silica fume is a relatively old additive, its amount as a supplementary material in concrete mixtures is not fully understood. More thorough investigations on the physical and chemical effects of silica fume should be conducted.

S. Kennouche researched self-compacting concrete and found that the best workability results could be achieved when 15 % of silica fume was added to cement [11]. Badr El-Din Ezzat Hegazy made bricks for an extremely aggressive environment and found that the best physical and mechanical properties could be achieved and when the mixture contained 25 % (by weight) of silica fume [12]. Dilip Kumar Singha worked with various types of concrete when $w/c = 0.45$ and noticed what workability, durability, strength, resistance to cracks could be improved with a combination of 6 % of metakaolin and 15 % (by weight) of silica fume [13]. S. Goberis in his research found that with deflocculation admixtures the content of microsilica could be reduced [14]. S. Bhanja tried to find the optimal amount of silica fume for tensile strength and found that the best compressive strength at 28 days was obtained with 5–10 % and the best flexural strength with 15–25 % of silica fume. The optimal value greatly depended on the water-to-binder ratio [15]. Yin-Wen Chan researched the effect of silica fume on steel fiber bond characteristics and found that 20–30 % (by weight) was the optimal amount for the best bond strength results [16]. H. Katkhuda also found that the optimal amount of silica fume strongly correlated with the water-to-binder ratio [17]. A. A. Elsayed in his experiment with slag cement found that high amounts of silica fume should be avoided, because the mixture slump intends to decrease, but its resistance to water penetration intends to increase [18]. Carsten Geisenhaunsluke noticed that the optimal amount of silica fume conformed with the lowest viscosity of the mixture [19]. Later, Michael Schmidt

confirmed this theory and has added that the maximum packing density correlates with the minimum viscosity of a concrete mixture [20]. Ivailo Terzijski has found that when the micro filler is substituted by the same amount of silica fume (by volume), the slump remains almost constant [21]. Melanie Shink [22] and Jennifer C. Scheydt [23] also found similar results. M. K. Maroliya in his research on the Reactive Powder concrete by the qualitative XRD analysis method found that the optimal amount of silica fume depended on the applied curing regime [24]. Detlef Heinz noticed that even if the thermal regime was applied, silica fume still reacted with portlandite, creating additional C-S-H phases [25]. J. Zelic investigated the effect of silica fume on cement kinetics and found that the addition of silica fume accelerated the initial rate of cement hydration, however, the pozzolanic reaction started only after 7 days of the hydration process [26]. Z. D. Rong investigated a cement-based composite with low water-to-binder ratio (≤0.35) and noticed that the unhydrated cement particles were surrounded with a high density C-S-H, low density C-S-H was hardly found [27]. An Cheng in his researched found that even a small addition of silica fume greatly reduced the porosity and hindered the leaching of calcium ions on cement-based materials [28].

According to the literature review, it is not entirely clear which amount of silica fume is optimal, how silica fume affects the hydration process; the literature is rich in reports on silica fume, however, most of the scientists are concentrated on workability and compressive strength. The purpose of this research is to extend the knowledge the workability and hydration process of ultra-high performance concrete affected by different amounts of silica fume. The better understanding of cement hydration could help not only in the field, but also save some cement and silica fume. For the investigation, slump, viscosity, the qualitative and quantitative XRD analysis and compression strength test methods were applied. Only pencil marks of page numbers should be used.

Materials and methods

Cement. Portland cement CEM I 52.5 R was used in the experiments. The main properties of this cement were as follows: the paste of normal consistency makes up 28.5 %; specific surface (by Blaine) equals 4840 cm^2/kg; the soundness (by Le Chatelier) measures 1.0 mm; the setting time (initial/final) is 110/210 min; the compressive strength (after 2/28 days) was found to be 32.3/63.1 MPa. The mineral composition could be quantitatively expressed as C_3S – 68.70 %, C_2S – 8.70 %, C_3A – 0.20 %, C_4AF – 15.90 %. The particle size distribution is shown in Fig. 1.

Silica fume. Main properties: density – 2532 kg/m^3; bulk density – 400 kg/m^3; *pH* – 5.3. The particle size distribution is also shown in Fig. 1.

Quartz powder. In the experiments, the quartz powder was used. The main properties of quartz powder are as follows: the density equals 2671 kg/m^3; the bulk density is 900 kg/m^3; the average particle size was found to be 18.12 μm; the specific surface (by Blaine) is 3450 cm^2/g. The particle size distribution is shown in Fig. 1.

Quartz sand. In the experiments, quartz sand was used. The main properties of quartz sand are: its fraction equals 0/0.5; its density is recorded as 2650 kg/m^3; the specific surface (by Blaine) numerical value is 91 cm^2/g.

Chemical admixture. In the experiments, a superplasticizer (SP) based on polycarboxylic ether (PCE) polymers with the following main properties was used: its appearance was – dark brown liquid, its specific gravity (20 °C) measured 1.08 ± 0.02 g/cm^3; the *pH* value was 7.0 ± 1; the viscosity was 128 ± 30 Pa·s; it had the 65.0 % alkali content and the 60.1 % chloride content.

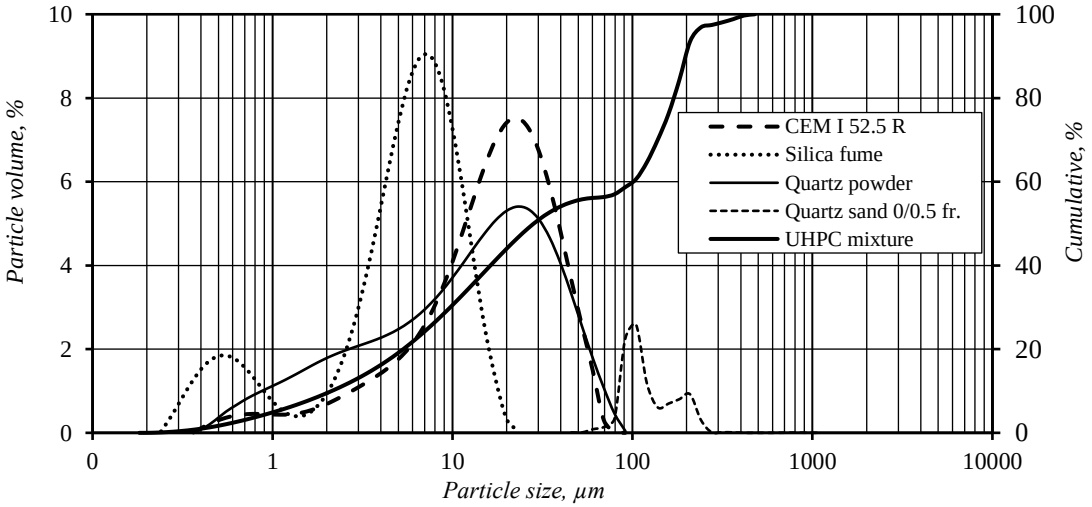

Fig. 1. Particle size distribution in Portland cement, silica fume, quartz powder, 0/0.5 fr. quartz sand and UHPC mixture

Specific surface and particle size distribution. Specific surface was measured with a Blaine instrument according to the EN 196-6:2010 standard [29]. Particle size distribution was measured with a Mastersize 2000 instrument produced by the Malvern Instruments Ltd.

Mixing, sample preparation and curing. Fresh concrete mixes were prepared with an EIRICH R02 mixer. Its main properties: capacity – 10 litres; mixing pan 0.55 and 1.00 kW; rotor power requirement and speed depend on the material mix (0.5–4.0 kW). The mixtures were prepared from dry aggregates. The cement and the aggregates were

dosed by weight, while water and chemical admixtures were added by volume. Cylinders (d = 50 mm, h = 50 mm) were formed for the research in order to determine the properties of concrete. Homogeneous mixes were cast in moulds and stored for 24 h at 20 C/95 RH (without compaction). After 24 h thermal treatment (1 + 18 + 3) was applied, and during the remaining time till the end of the 28-day period the specimens were stored under water at 20 °C.

Table 1. Chemical composition of Portland cement and silica fume

Components	Quantity, %	
	CEM I 52,5 R	Silica fume
SiO_2	20.61	92.08
TiO_2	-	-
Al_2O_3	5.45	1.16
Fe_2O_3	3.36	1.24
MnO	-	-
MgO	3.84	0.80
CaO	63.42	1.07
SO_3	0.80	1.27
Na_2O	0.20	1.13
K_2O	1.00	0.67
P_2O_5	-	-
$Na_2O_{eq.}$	0.86	1.57
Loss of ignition	1.00	-

Cement paste hydration temperature. The cement paste hydration temperature was measured according to the EN 196-9:2010 standard [32]. Cement pastes were prepared with the water-to-binder ratio W/B = 0.30. Measurements were performed with a TC-08 thermocouple data logger and a type K thermocouple. The main specification of the TC-08 data logger: the number of channels – 8; measures from -270 °C to +1820 °C; temperature accuracy ±0.2 °C.

Table 2. Mixing procedure of UHPC

Time, s	Mixing procedure
60	Homogenization of silica fume, cement, quartz powder and quartz sand
30	Addition of 100 % of water and 50 % of superplasticizer
60	Homogenization
120	Pause
30	Addition of the remaining superplasticizer
60	Homogenization

Slump and viscosity. Slump was measured according to the EN 1015-3:1999 standard (without compaction) [30]. Dynamic viscosity was measured by the falling ball method (modified Stokes method) described in [31].

Sample preparation for XRD analysis. Hardened cement pastes with 0 %, 10 %, 15 % and 20 % of silica fume were used for the XRD analysis. The XRD measurements were performed with an XRD 3003 TT diffractometer of GE Sensing & Inspection Technologies GmbH with θ-θ configuration and CuKα radiation (λ = 1.54 Å). The angular range was from 5 to 70° 2θ with a step width of 0.02° and a measuring time of 6 sec/step. For XRD quantitative phase analysis using the Rietveld refinement, the samples were mixed with 20 wt.% ZnO (a standard material widely used in the XRD analysis) as an internal standard and stored in the argon atmosphere until measurement. This permits estimating the amount of non-crystalline phases by the Rietveld fitting procedure.

Table 3. Activation method of UHPC

Notation	Description
T20	Without heat treatment, after the demoulding specimens were stored for 27 days in 20 °C water
T80	After demoulding, the specimens were stored for 24 hours in 80 °C water (3+16+5) and for the rest of time were left in 20 °C water

Density and compressive strength. Density and compressive strength were measured from 6 cylinders (d = 50 mm; h = 50 mm) as the average value. Density was measured according to the EN 12390-7:2009 standard [33] and compressive strength according to the EN 12390-4:2003 standard [34].

Results and discussion

According to the methods described above, four compositions of UHPC with different amounts of silica fume were created (Table 4). $0SiO_2$/100QP is the reference composition without silica fume, $10SiO_2$/90QP when 10 % of quartz powder is substituted by silica fume, $15SiO_2$/85QP when 15 % of quartz powder is substituted by silica fume, and $20SiO_2$/80QP when 20 % of quartz powder is substituted by silica fume. The main goal of the experiment was to find out how different amounts of silica fume affects the workability and hydration process of UHPC. For the investigation, the slump test, modified stokes, the semi-adiabatic, qualitative and quantitative XRD analysis, the density and compressive test methods were applied.

Table 4. Composition of ultra-high performance concrete

Composition	Amount of silica fume, %	Water, l	Cement, kg/m^3	W/C	Microfiller, kg/m^3		Quartz sand, kg/m^3	Superplasticizer, l
					Silica fume	Quartz powder		
$0SiO_2$/100QP	0	224	735	0.30	-	511	962	36.75
$10SiO_2$/90QP	10				74	438		
$15SiO_2$/85QP	15				110	401		
$20SiO_2$/80QP	20				147	364		

Slump and dynamic viscosity

An interesting fact was noted that when silica fume was added to the UHPC composition from 0 % to 20 % (by weight), the slump in all compositions remained almost constant (~37.5 ± 0.5 cm). The substitution degree of quartz powder by silica fume did not affect the slump of the UHPC mixture (Fig. 2).

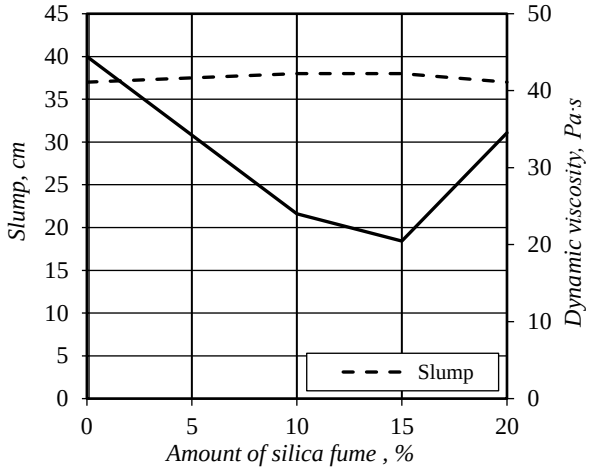

Fig. 2. Influence of silica fume on the slump and dynamic viscosity of UHPC

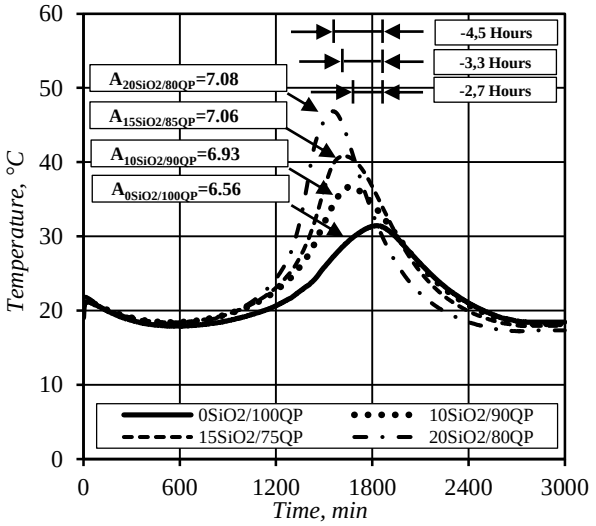

Fig. 3. Influence of silica fume on cement paste hydration temperature

However, the dynamic viscosity was affected dramatically: viscosity decreased more than by half – from 44 Pa·s ($0SiO_2$/100QP) to 20 Pa·s ($15SiO_2$/QP85). The lowest dynamic viscosity was obtained in the composition ($15SiO_2$/QP85) when 15 % of the quartz powder was substituted by silica fume. The lowest dynamic viscosity probably related with the best particle size distribution and the maximum packing density. Maximum packing within the cement particles reduces the wall effect in the transition zone between the paste and the microfiller, giving a denser, more homogeneous and uniform UHPC mixture.

Cement paste hydration temperature

Figure 3 shows the effects of different amounts of silica fume on the cement pastes (*W/B* = 0.30) hydration temperature development. Interesting by with an increased amount of silica fume the cement hydration rate and temperature increased.

When the quartz powder was substituted from 0 % to 20 % by the silica fume, the hydration temperature increased by about 50 % – from 31.44 °C ($0SiO_2$/100QP) to 46.86 °C ($20SiO_2$/80QP), the hydration rate increased by about 15 %, and the final hardening was reduced by 4.5 hours ($20SiO_2$/80QP).

The area under the temperature curve can be attributed to heat flux during the hydration process (Table 5). It could be noted that in compositions with silica fume the area under the temperature line was almost similar (~7.0 relative units). So, it could be concluded, that a higher amount of silica fume only accelerates the cement paste initial hydration process; however, the final strength is affected negligibly, and the further strength gain is mostly due to the on-going pozzolanic reaction.

The accelerated hydration rate and the increased hydration temperature probably could be explained by two phenomena: the dissolved silica fume produces a weak silicic acid which accelerates the dissolution of the clinker mineral and, being a relatively small silica fume, generates nucleation sites for the precipitation of hydration products.

Qualitative and quantitative XRD analysis

Figure 4 illustrates the XRD patterns of four hardened cement pastes with different amounts of silica fume when no heat treatment was applied. The CH phase was found at *d* equalling 0.3042; 0.2789 and 0.1924 nm. Evidently, the crystalline phase of CH was decreased with an increased amount of the silica fume. C_2S was found at the following levels of *d*: 0.2790, 0.2783, 0.2745, 0.2645, 0.2610, 0.2189 nm, while C_3S phases were found at *d* equalling 0.3036, 0.2773, 0.2748, 0.2604, 0.2181 nm. It was noticed that with increased amounts of silica fume decreased the intensity of C_2S and C_3S phases. The decreased C_2S and C_2S peaks were probably related with the better solubility of the clinker phase, and the decreased CH peaks were related with the consumption by silica fume.

Table 5. Cement paste hydration parameters

Composition	Initial hardening, min	Final hardening, min	Initial temperature, °C	Minimal temperature, °C	Maximal temperature, °C	Area, relative units
$0SiO_2$/100QP	548	1825	21.08	17.90	31.44	6.56
$10SiO_2$/90QP	505	1664	21.08	18.41	36.67	6.93
$15SiO_2$/75QP	504	1626	21.08	18.39	40.84	7.06
$20SiO_2$/80QP	502	1554	21.08	18.19	46.86	7.08

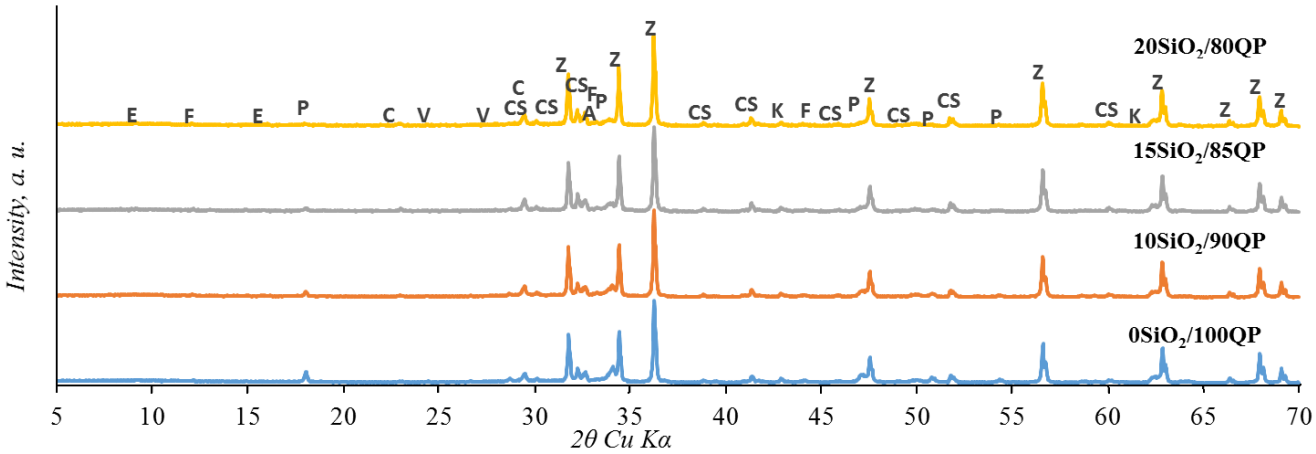

Fig. 4. XRD patterns of hardened cement pastes cured for 28 days at 20 °C. P – portlandite; K – periclase; C – calcite; E – ettringite; Z – ZnO (internal standard); CS – C_3S and C_2S; V – vaterite, A – C_3A; F – C_4AF.

Figures 5 and 6 illustrate the XRD quantitative analysis of four hardened cement pastes with different amounts of the silica fume. Experiment results revealed that the clinker phases in the specimens continued to react with water-forming amorphous phases and portlandite. Silica fume reacted with portlandite to form additional C-S-H phases. When heat treatment was not applied (Fig. 5 and Table 6) and the silica fume was increased up to 20 % (by weight), the portlandite phase decreased from 11.9 % ($0SiO_2$/100GP-T20) to 3.7 % ($20SiO_2$/80GP-T20) and the amorphous phase increased from 36.9 % to 47.1 % respectively.

When heat treatment was applied (Fig. 6 and Table 6) and silica fume was increased up to 20 % (by weight), the portlandite phase decreased from 13.6 % ($0SiO_2$/100GP-T80) to 0.0 % ($20SiO_2$/80GP-T80), and the amorphous phase respectively increased from 40.9 % to 47.5 %. The contents of the main hydration products are listed in Table 6. One can see that there is a large quantity of unhydrated cement due to the low *W/B* ratio. The remained cement quantity correlates with the cement paste hydration temperature. The XRD analysis revealed that cement pastes with different amounts of silica fume had a positive effect on the portlandite consumption. Portlandite makes an inhomogeneous microstructure, which had a negative effect on the compressive strength. The reduced portlandite compressive strength can increase due to formation in a less porous transition zone and formation of additional C-S-H. However, the applied thermal treatment and the addition of 20 % of silica fume consumed all portlandite, verifying that in the researched composition ($20SiO_2$/80GP-T80) the 20 % substitution of quartz powder by silica fume was not economical.

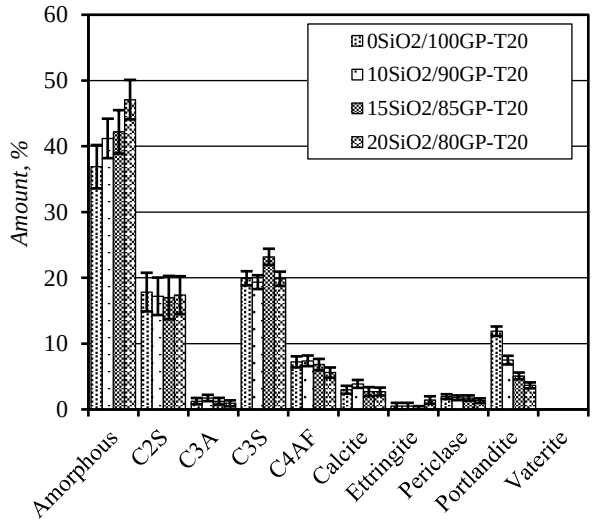

Fig. 5. Mineralogical composition of the binder for UHPC when heat treatment was not applied

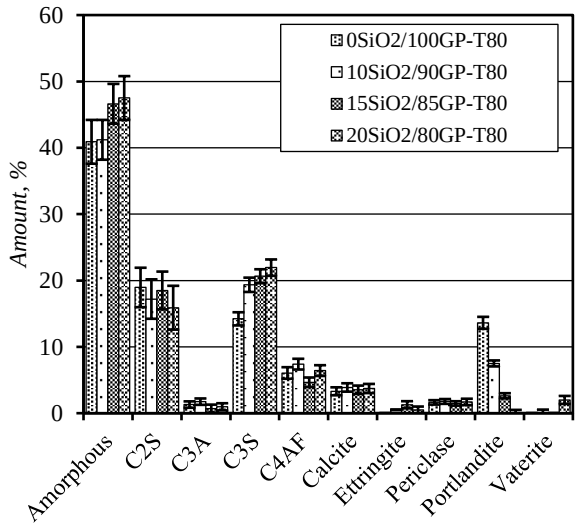

Fig. 6. Mineralogical composition of the binder for UHPC when heat treatment was applied

Table 6. Mineralogical composition of the binder for UHPC with and without heat treatment

Composition		Phases									
		Amorphous	C_2S	C_3A	C_3S	C_4AF	Calcite	Ettringite	Periclase	Portlandite	Vaterite
$0SiO_2$/100GP-T20	wt.%	36.9	17.8	1.3	19.9	7.2	3.0	0.5	2.0	11.9	0.0
	σ, %	3.3	2.9	0.5	1.1	0.8	0.6	0.5	0.4	0.7	0.0
$0SiO_2$/100GP-T80	wt.%	40.9	19.0	1.3	14.2	6.1	3.3	0.0	1.6	13.6	0.0
	σ, %	3.3	3.0	0.5	1.0	0.9	0.6	0.0	0.3	0.9	0.0
$10SiO_2$/90GP-T20	wt.%	41.2	17.2	1.7	19.4	7.4	3.9	0.5	1.8	7.5	0.0
	σ, %	3.0	2.9	0.5	1.1	0.8	0.6	0.5	0.4	0.7	0.0
$10SiO_2$/90GP-T80	wt.%	43.1	17.9	1.2	19.1	6.4	3.8	0.0	1.6	4.5	2.4
	σ, %	3.0	3.0	0.5	1.1	0.8	0.6	0.0	0.4	0.5	0.5
$15SiO_2$/85GP-T20	wt.%	42.2	17.0	1.3	23.2	6.8	2.7	0.0	1.7	5.1	0.0
	σ, %	3.3	3.3	0.5	1.2	0.9	0.7	0.5	0.4	0.5	0.0
$15SiO_2$/85GP-T80	wt.%	46.6	18.5	0.7	20.6	4.7	3.5	1.3	1.5	2.6	0.0
	σ, %	3,0	2.9	0.6	1.1	0.7	0.6	0.5	0.3	0.4	0.0
$20SiO_2$/80GP-T20	wt.%	47.1	17.4	0.9	19.9	5.6	2.7	1.4	1.3	3.7	0.0
	σ, %	3.0	2.9	0.5	1.1	0.8	0.6	0.6	0.4	0.5	0.0
$20SiO_2$/80GP-T80	wt.%	47.5	15.9	1.0	21.9	6.4	3.7	0.5	1.7	0.0	2.0
	σ, %	3.3	3.3	0.5	1.2	0.8	0.7	0.5	0.5	0.5	0.6

Density and compressive strength

As was expected, the density of the UHPC composition with and without heat treatment when different amounts of quartz powder was substituted by silica fume remained almost constant and was about 2400 kg/m^3 (Fig. 7 and Table 7). The lowest density was obtained in the reference composition ($0SiO_2$/100QP) without silica fume, and the highest density was obtained in the composition ($15SiO_2$/85QP) when 15 % of quartz powders were substituted by silica fume. These results correlate with the highest and the lowest viscosity.

An interesting fact was noticed that portlandite consumption by silica fume was the highest in the composition ($20SiO_2$/80GP-T80) with 20 % (by weight) of silica fume; however, the best compressive strength result was obtained in the composition ($15SiO_2$/85GP-T80) with 15 % (by weight) of silica fume, probably due to a better particle size distribution and the obtained densest structure.

When the heat treatment was not applied, the compressive strength increased by about 34 % – from 95 MPa ($0SiO_2$/100QP) to 127 MPa ($15SiO_2$/85QP). When heat treatment was applied, the compressive strength increased by about 47 % – from 96 MPa ($0SiO_2$/100QP) to 141 MPa ($15SiO_2$/85QP). These results correlate with the lowest viscosity and the highest density of UHPC.

In the experiment it has been noticed that silica fume reacts with calcium hydroxide to produce additional calcium silicate hydrates (C-S-H); thus, the compressive strength of concrete increases; however, since silica fume has a very high surface area, high amounts ≥15 % (by weight) of silica fume are not desirable for a good-workability concrete, because water requirements for the normal consistency mixture and viscosity tend to increase.

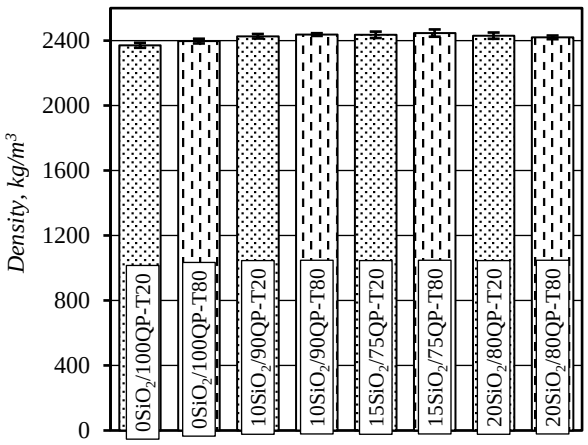

Fig. 7. The density of UHPC with and without heat treatment

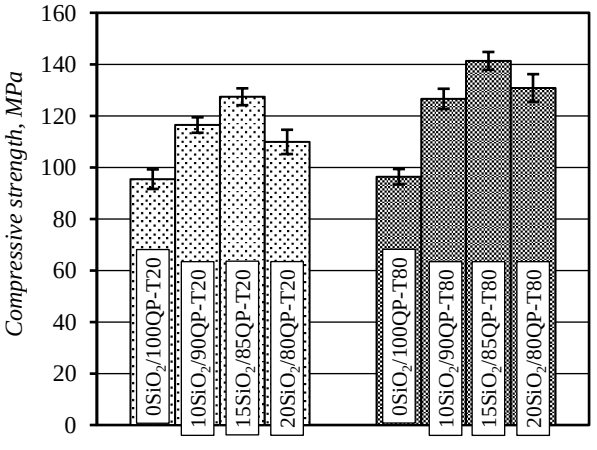

Fig. 8. The compressive strength of UHPC with and without heat treatment

Table 7. Physical and mechanical properties of UHPC

Parameter	Composition			
	0SiO_2/100QP	10SiO_2/90QP	15SiO_2/85QP	20SiO_2/80QP
Slump, cm	37	38	38	37
Viscosity, Pa·s	44	24	20	35
Density, kg/m^3 (without heat treatment)	2371	2427	2436	2431
Density, kg/m^3 (with heat treatment 3+16+5)	2397	2458	2446	2420
Compressive strength, MPa (without heat treatment)	95	116	127	110
Compressive strength, MPa (with heat treatment 3+16+5)	96	127	141	131

Another interesting fact was that the compressive strength after 28 days with thermal treatment as compared without thermal treatment was not significantly increased. However, the amount of portlandite was reduced drastically, and this means that the 28-day thermal treatment for compressive strength is not efficient. Better particle size distribution has a more positive effect on workability and compressive strength. However, the increased amount of silica fume not necessarily gives the densest structure; it has a positive effect on the further hydration, but due to the decreased workability an inhomogeneous structure formation could be expected.

Conclusions

An extensive experiment was carried out to determine the silica fume effect on the ultra-high-performance concrete. The following conclusions can be derived from the present investigation:

1. When the quartz powder was replaced from 0 % to 20 % by silica fume, slump all the time remained almost constant and was about 37.5 ± 0.5 cm. The lowest viscosity of the ultrahigh performance concrete was achieved when the quartz powder was by 15 % replaced by silica fume, and it was 20 Pa·s.
2. The semi-adiabatic method revealed that the hydration rate and temperature of the cement paste tended to increase with the increased amount of silica fume.
3. Regardless of the selected thermal treatment, the lowest amount of portlandite was detected in hardened cement samples with the 20 % addition of silica fume. When no heat treatment was applied, portlandite was detected 3.7 % (by weight) and 0.0 % (by weight) with heat treatment.
4. Best compressive strength results at 28 days fallows almost the same trend as lowest viscosity of ultrahigh performance concrete mixture. When heat treatment was not applied and quartz powder was replaced by 15 % of silica fume compressive strength was obtained 127 MPa and 141 MPa with heat treatment.

References

1. LST EN 206-1:2002. Concrete – Part 1: Specification, performance, production and conformity.
2. **Singh L. P., Karade S. R., Bhattacharyya S. K., Yousuf M. M., Ahalawat S.** Beneficial role of nanosilica in cement based materials – A review // Construction and Building Materials. 2013. Vol. 47. P. 1069–1077. http://dx.doi.org/10.1016/j.conbuildmat.2013.05.052
3. **Dils J., Boel V., De Schutter G.** Influence of cement type and mixing pressure on air content, rheology and mechanical properties of UHPC // Construction and Building Materials. 2013. Vol. 41. P. 455–463. http://dx.doi.org/10.1016/j.conbuildmat.2012.12.050
4. **Yu R., Spiesz P., Brouwers H. J. H.** Mix design and properties assessment of Ultra-High Performance Fibre Reinforced Concrete (UHPFRC) // Cement and Concrete Research. 2014. Vol. 56. P. 29–39. http://dx.doi.org/10.1016/j.cemconres.2013.11.002
5. **Arroudj K., Zenati A., Oudjit M. N., Bali A., Hamou A. T.** Reactivity of fine quartz in presence of silica fume and slag // Engineering. 2011. Vol. 3. P. 569–576. http://dx.doi.org/10.4236/eng.2011.36067
6. **Maroliya M. K.** Micro structure analysis of reactive powder concrete // International Journal of Engineering Research and Development. 2012. Vol. 4. N 2. P. 68–77.
7. **Cao J., Chung D. D. L.** Microstructural effect of the shrinkage of cement-based materials during hydration, as indicated by electrical resistivity measurement // Cement and Concrete Research. 2004. Vol. 34. P. 1893–1897. http://dx.doi.org/doi:10.1016/j.cemconres.2004.02.002.
8. **Sounthararajan V. M., Srinivasan K., Sivakumar A.** Micro filler effects of silica-fume on the setting and hardened properties of concrete // Research Journal of Applied Sciences, Engineering and Technology. 2013. Vol. 6 (14). P. 2649–2654.
9. **Dotto J. M. R., Abreu A. G., Dal Molin D. C. C., Muller I. L.** Influence of silica fume addition on concretes physical properties and on corrosion behaviour of reinforcement bars // Cement and Concrete Composites. 2004. Vol. 26. P. 31–39. http://dx.doi.org/10.1016/S0958-9465(02)00120-8
10. **Kocak Y.** A study on the effect of fly ash and silica fume substituted cement paste and mortars // Scientific Research and Essays. 2010. Vol. 5 (9). P. 990–998.
11. **Kennouche S., Zerizer A., Benmounah A., Hami B., Mahdad M., Benouali H., Bedjou S.** Formulation and characterization of self compacting concrete with silica fume // Journal of Engineering and Technology Research. 2013. Vol. 5(5). P. 160–169. http://dx.doi.org/10.5897/JETR2013.0306
12. **Hegazy B. El-D. E., Fouad H. A., Hassanain A. M.** Incorporation of water sludge, silica fume, and rice husk ash in brick making // Advances in Environmental Research. 2012. Vol. 1. N 1. P. 83–96. http://dx.doi.org/10.12989/aer.2012.1.1.083
13. **Roy D. K. S., Sil A.** Effect of partial replacement of cement by silica fume on hardened concrete // International Journal of Emerging Technology and Advanced Engineering. 2012. Vol. 2. N 8. P. 472–475.
14. **Goberis S., Pundienė I.** Some aspects of influence of microsilica and admixtures on hydration kinetics of the alumina cement "Gorkal-40" // Materials science (Medžiagotyra). 2004. Vol. 10. N 1. P. 50–54.
15. **Bhanja S., Sengupta B.** Influence of silica fume on the tensile strength of concrete // Cement and Concrete Research. 2005. Vol. 35. P. 743–747.

http://dx.doi.org/10.1016/j.cemconres.2004.05.024
16. **Chan Y. W., Chu S. H.** Effect of silica fume on steel fiber bond characteristics in reactive powder concrete // Cement and Concrete Research. 2004. Vol. 34. P. 1167–1172. http://dx.doi.org/10.1016/j.cemconres.2003.12.023
17. **Katkhuda H., Hanayneh B., Shatarat N.** Influence of silica fume on high strength lightweight concrete // International Science Index, Civil and Environmental Engineering. 2009. Vol. 3. N 10. P. 407–414.
18. **Elsayed A.** Influence of silica fume, fly ash, super pozz, and high slag cement on water permeability and strength of concrete // Concrete Research Letters. 2012. Vol. 3. N 4. P. 528–540.
19. **Geisenhaunsluke C., Schmidt M.** Methods for modelling and calculation of high density packing for cement and fillers in UHPC // Ultra High Performance Concrete (UHPC), International Symposium on Ultra High Performance Concrete, Kassel University Press, Kassel, 2004. P. 303–312.
20. **Schmidt M., Fehling E.** Ultra-high-performance concrete: research, development and application in Europe // 7th International Symposium on the Utilization of High-Strength and High-Performance-Concrete, ACI Washington, 2005. P. 51–78.
21. **Terzijski I.** Compatibility of components of high and ultra high performance concrete // Ultra High Performance Concrete (UHPC) proceedings of the International Symposium on Ultra High Performance Concrete, Kassel, Germany, 2004. P. 175–186.
22. **Shink M., Vacher J. P.** EFFIC design properties and application of a creative concrete // Ultra High Performance Concrete (UHPC) proceedings of the Second Internationals Symposium on Ultra High Performance Concrete, Kassel, Germany, 2008. P. 847–854.
23. **Scheydt J. C., Herold G., Muller H. S., Kuhnt M.** Development and application of UHPC convenience blends // Ultra High Performance Concrete (UHPC) Proceedings of the Second Internationals Symposium on Ultra High Performance concrete, Kassel, Germany, 2008. P. 69–76.
24. **Maroliya M. K.** A qualitative study of reactive powder concrete using X-Ray diffraction technique // IOSR Journal of Engineering (IOSRJEN). 2012. Vol. 2. N 9. P. 12–16. http://dx.doi.org/10.9790/3021-02911216
25. **Heinz D., Urbonas L., Gerlicher T.** Effect of heat treatment method on the properties of UHPC // Ultra-High Performance Concrete and Nanotechnology in Construction. Proceedings of Hipermat 2012 3th International Symposium on UHPC and Nanotechnology for High Performance Construction Materials, Kassel, 2012. P. 283–290.
26. **Zelic J., Rušic D., Veža D., Krstulovic R.** The role of silica fume in the kinetics and mechanisms during the early stage of cement hydration // Cement and Concrete Research. 2000. Vol. 30. N 10. P. 1655–1662. http://dx.doi.org/10.1016/S0008-8846(00)00374-4
27. **Rong Z. D., Sun W., Xiao H. J., Wang W.** Effect of silica fume and fly ash on hydration and microstructure evolution of cement based composites at low water–binder ratios // Construction and Building Materials. 2014. Vol. 51. P. 446–450. http://dx.doi.org/10.1016/j.conbuildmat.2013.11.023
28. **A. Cheng, Chao S. J., Lin W. T.** Effects of leaching behavior of calcium ions on compression and durability of cement-based materials with mineral admixtures // Materials. 2013. Vol. 6. P. 1851–1872. http://dx.doi.org/10.3390/ma6051851
29. EN 196-6:2010. Methods of testing cement – Part 6: Determination of fineness.
30. EN 1015-3:1999/A2:2006. Methods of test for mortar for masonry - Part 3: Determination of consistence of fresh mortar (by flow table).
31. **Vaitkevičius V., Šerelis E., Lygutaitė R.** Production waste of granite rubble utilisation in ultra high performance concrete // Journal of Sustainable Architecture and Civil Engineering. 2013. Vol. 2. N 3. P. 54–60. http://dx.doi.org/10.5755/j01.sace.2.3.3873
32. EN 196-9:2010. Methods of testing cement – Part 9: Heat of hydration – semi-adiabatic method.
33. EN 12390-7:2009. Testing hardened concrete – Part 7: Density of hardened concrete.
34. LST EN 12390-4:2003. Testing hardened concrete – Part 4: Compressive strength – specification for testing machines.

E. Šerelis, V. Vaitkevičius, V. Kerševičius

SILICIO MIKRODULKIŲ ĮTAKA YPAČ STIPRAUS BETONO TECHNOLOGINĖMS SAVYBĖMS IR HIDRATACIJOS PROCESUI

S a n t r a u k a

Straipsnyje nagrinėjama silicio mikrodulkių įtaka ypač stipraus betono technologinėms savybėms ir portandcemenčio hidratacijos procesui. Eksperimentiniuose tyrimuose panaudotos silicio mikrodulkės, esančios ferosilicio lydinių gamybos atlieka. Silicio mikrodulkės gali būti tinkamai utilizuotos gaminant ypač stiprius betonus, tačiau, atlikus išsamią literatūros analizę, pastebėta, jog nėra iki galo aiškų, koks optimalus silicio mikrodulkių kiekis gaminant ypač stiprius betonus, taip pat nėra iki galo aišku, kaip silicio mikrodulkės paveiks cemento hidratacijos procesą esant mažiems *V/C* santykiams. Nors pasaulinėje praktikoje atlikta daugybė eksperimentinių tyrimų su silicio mikrodulkėmis, tačiau daugelis autorių susikoncentravę aiškinant ne technologinių ir mechaninių savybių kitimą, o jų priežastingumą. Straipsnio pagrindinis tikslas – praplėsti jau žinomas žinias apie silicio mikrodulkių įtaka ir jas pritaikyti gaminant ypač stiprius betonus. Eksperimentiniams tyrimams atlikti buvo pritaikyti šie metodai: slankumo, dinaminės klampos, kokybinės ir kiekybinės rentgenografinės analizės ir gniuždymo stiprio. Atliekant tyrimus, buvo nustatyta, jog, naudojant silicio mikrodulkes, rišimosi laiką galima sutrumpinti apie 4,4 h, o gniuždymo stiprį padidinti apie 30 % nuo 95 MPa iki 127 MPa.

Reikšminiai žodžiai: gniuždymo stipris, silicio mikrodulkės, ypač stiprus betonas, rentgenografinė analizė.